



Constraining CP violating operators in charged and neutral triple gauge couplings

Anke Biekötter^{a,b,*}, Parisa Gregg^{a,b}, Frank Krauss^{a,b}, Marek Schönherr^a

^a Institute for Particle Physics Phenomenology, Durham University, United Kingdom

^b Institute for Data Science, Durham University, United Kingdom

ARTICLE INFO

Article history:

Received 4 March 2021

Received in revised form 15 April 2021

Accepted 19 April 2021

Available online 22 April 2021

Editor: G.F. Giudice

ABSTRACT

We constrain CP -violating charged and neutral anomalous triple gauge couplings using LHC measurements and projections of diboson and VBF Vjj production, both with subsequent leptonic decays. For triple gauge couplings involving W bosons we analyse differential asymmetries and interpret our results in the SMEFT at dimension-six. For neutral triple gauge couplings, which are dominantly constrained by high transverse-momentum bins, we present the resulting bounds in terms of a general anomalous couplings framework.

© 2021 The Author(s). Published by Elsevier B.V. This is an open access article under the CC BY license (<http://creativecommons.org/licenses/by/4.0/>). Funded by SCOAP³.

1. Introduction

The observation of the Higgs boson in 2012 [1,2] has been a milestone in the confirmation of electroweak symmetry breaking (EWSB). Since, apart from fixing the Higgs couplings, the mechanism of EWSB also predicts the interactions of the electroweak gauge bosons, precise measurements of the triple gauge couplings (TGCs) play a crucial role in experimentally testing the SM. CP -violating interactions of the gauge bosons are of particular relevance in this regard, since they provide additional sources of CP violation, necessary to describe, for example, electroweak baryogenesis [3–7].

In our work, we study CP -odd anomalous triple gauge couplings involving two (charged) W bosons, WWZ and $WW\gamma$, as well as interactions of neutral gauge bosons, ZZZ , $ZZ\gamma$ and $Z\gamma\gamma$, which are completely absent in the SM. For charged anomalous triple gauge couplings, we consider constraints from the measurement of the channels $WW \rightarrow \ell\ell\nu\nu$ [8], $WZ \rightarrow \ell^+\ell^-\ell^\pm\nu$ [9], $W\gamma \rightarrow \ell^\pm\nu\gamma$ [10], as well as $Zjj \rightarrow \ell^+\ell^-jj$ [11] and $Wjj \rightarrow \ell\nu jj$ production [12]. To describe small deviations from the Standard Model (SM) values of the charged TGCs in a model-independent fashion, we will use the language of Standard Model Effective Field Theory (SMEFT) [13–17], where CP -odd SMEFT operators influencing the charged TGCs appear at dimension six. Constraints on these operators have been studied and constrained in Higgs boson [18–23] and diboson production processes [24–28] as well as vector boson scattering [29]. Recently, CP violation in diboson pro-

duction has also been studied in Ref. [30]. We consider the same experimental inputs, but our analysis differs in the selection of observables sensitive to CP violation, using differential asymmetries rather than complete differential distributions, reducing both experimental and theoretical systematic uncertainties. Our study provides an independent confirmation of the results found in Ref. [30] using SHERPA for the generation of both the SM as well as the beyond SM events, and they also serve as independent validation of the implementation of this sector in SHERPA.

For neutral anomalous triple gauge couplings we consider constraints from the $ZZ \rightarrow 4\ell$ and $2\ell 2\nu$ final states [31,32] as well as $Z\gamma \rightarrow 2\ell\gamma$ and $2\nu\gamma$ production channels [33,34]. Due to the dominance of squared neutral triple gauge coupling (nTGC) contributions compared to the polarization-suppressed (linear) interference with the SM [25,35,36], we investigate their effects on the cross section in the high- p_T regime, rather than studying asymmetries.

2. Charged aTGC

SMEFT [13–17] provides a versatile framework to describe small deviations from the SM, such as those induced by anomalous triple gauge couplings. We restrict our analysis to dimension-six operators leading to CP violation in diboson production through a direct modification of the γWW and ZWW interactions. In the Warsaw basis [15], there are two operators which directly affect these vertices and the effective Lagrangian is given by

$$\mathcal{L} = \mathcal{L}_{\text{SM}} + \frac{c_{\tilde{W}}}{\Lambda^2} \mathcal{O}_{\tilde{W}} + \frac{c_{H\tilde{W}B}}{\Lambda^2} \mathcal{O}_{H\tilde{W}B}, \quad (1)$$

* Corresponding author.

E-mail address: anke.biekotter@durham.ac.uk (A. Biekötter).

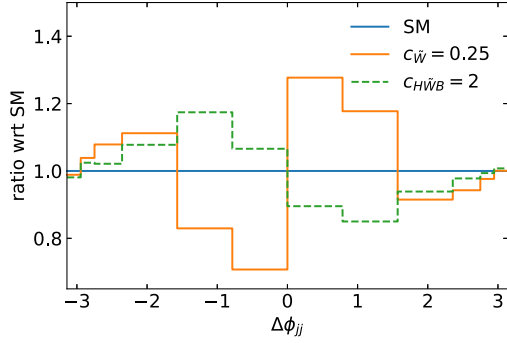


Fig. 1. $\Delta\phi_{jj}$ distribution for the Zjj analysis.

where \mathcal{L}_{SM} is the SM Lagrangian, Λ denotes the new physics scale and the c_i are the Wilson coefficients of the operators

$$\begin{aligned} \mathcal{O}_{\tilde{W}} &= \epsilon^{IJK} \tilde{W}_{\mu}^{I\nu} W_{\nu}^{J\rho} W_{\rho}^{K\mu}, \\ \mathcal{O}_{H\tilde{W}B} &= H^{\dagger} \tau^I H \tilde{W}_{\mu\nu}^I B^{\mu\nu}. \end{aligned} \quad (2)$$

The operator $\mathcal{O}_{H\tilde{W}B}$ also affects Higgs-gauge couplings and its Wilson coefficient can thus be constrained independently through Higgs sector observables.

In the following, we calculate and combine the constraints on the Wilson coefficients $c_{H\tilde{W}B}$ and $c_{\tilde{W}}$ from WW , WZ , $W\gamma$ and VBF Zjj and Wjj production at the LHC. For each considered channel i , we study the differential distributions of an angle ζ_i which is defined from the triple products or, equivalently, the difference in azimuthal angle of the rapidity-ordered final-state (pseudo-)particles k and l , e.g. $\Delta\phi_{kl} \propto \sin^{-1}((\vec{p}_k - \vec{p}_l)_z (\vec{p}_k \times \vec{p}_l)_z)$. The operators $\mathcal{O}_{\tilde{W}}$ and $\mathcal{O}_{H\tilde{W}B}$ produce modulations in these distributions. As an example, we display the $\Delta\phi_{jj}$ distribution for the two tagging jets in Zjj production in Fig. 1.

We divide each of these $\Delta\phi$ distributions into six pairs of bins using the boundaries $\pm[0, \frac{1}{4}, \frac{1}{2}, \frac{3}{4}, \frac{7}{8}, \frac{15}{16}, 1] \cdot \pi$ and construct six asymmetries A_{ij} between the number N of events in corresponding bins at positive or negative $\Delta\phi$, i.e. we compare the number of events in the bin $[-\frac{\pi}{4}, 0]$ with the number of events in the bin $[0, \frac{\pi}{4}]$ and so on:

$$A_{ij} = \frac{N_{i,-j} - N_{i,+j}}{N_{i,-j} + N_{i,+j}}, \quad (3)$$

$$i = WW, WZ, W\gamma, Zjj, Wjj, \quad j = 1, \dots, 6.$$

In the above, $N_{i,j}$ corresponds to number of events in bin j of the $\Delta\phi$ distribution for channel i . The resulting differential asymmetries A_{ij} are defined such that they vanish exactly for the SM and SM backgrounds, where no CP violation is present.¹ As a reference, we display the asymmetries generated by $c_{\tilde{W}}$ in the Zjj channel and by $c_{H\tilde{W}B}$ in the $W\gamma$ channel in Fig. 2. For the Zjj channel large asymmetries are generated which come with rather large uncertainties, while for the $W\gamma$ channel both the asymmetries and their uncertainties are smaller. The inclusion of bin-wise asymmetries, which we use here for the first time, with respect to global asymmetries over the full $\Delta\phi$ range has the advantage that more than one direction in the $c_{\tilde{W}}-c_{H\tilde{W}B}$ plane can be tested. Moreover, this allows us to trade off better statistics for larger generated asymmetries in a constrained phase-space region, compare Fig. 2. Generally, an advantage of asymmetries is that systematic uncertainties largely cancel in the ratio. Since the limits are therefore

¹ The CP violation present in the SM has been checked to be negligible for the range of observables and coefficients considered in this letter.

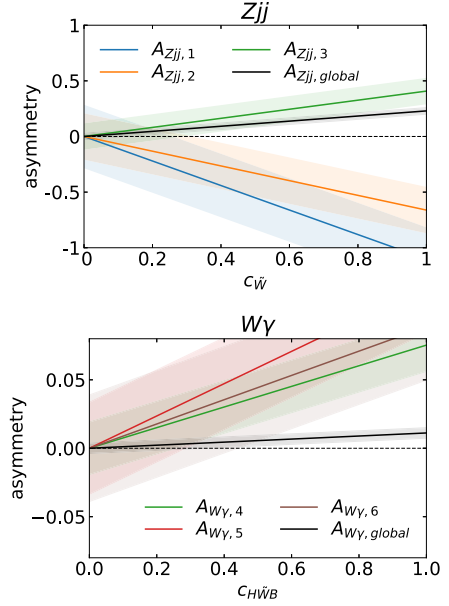


Fig. 2. Dominant bin-wise asymmetries as defined in Eq. (3) for the Zjj (top) and the $W\gamma$ (bottom) channels. The shaded bands reflect the 2σ uncertainty band on the asymmetry from statistics and background subtraction. The selected channels result in the strongest bounds on $c_{\tilde{W}}$ and $c_{H\tilde{W}B}$ respectively. The global asymmetry, which is not used in this paper, is defined using the full $\Delta\phi$ phase space.

entirely determined by the statistical uncertainties, we do not consider any systematic uncertainties here. The only exemption from this are uncertainties from background subtraction which can be relevant for channels with a small signal-over-background ratio. For channels with $S/B < 1$, we take therefore into account the uncertainty from background subtraction as $\sigma_{A_{ij}}^{\text{bkg}} = \sqrt{N_{ij}^{\text{bkg}}/N_{ij}^{\text{sig}}}$. For the WZ , $W\gamma$ and WW channels, for which $S/B > 1$, we have explicitly checked that including the background uncertainty will influence the limits deduced by no more than 3%, 12% and 20% respectively.

We generate events at leading order (LO) with SHERPA-2.2.10 [37, 38] with the default NNPDF30_nnlo_as_0118 parton distribution function [39] from LHAPDF 6.2.1 [40]; matrix elements are calculated with COMIX [41] and parton showered with CSSHOWER [42]. QED corrections are effected through a YFS soft-photon resummation [43,44]. For multi-parton interactions, hadronization, and subsequent hadron decays we use the SHERPA default settings. EFT contributions are generated using the SMEFTsim model [45] in SHERPA through its UFO [46] interface [47]. We consider the interference of the SM with the dimension-six operator only and neglect contributions from the squares of dimension-six terms.

In each channel, we normalize the SM cross section to the experimentally observed cross section and assume identical normalization factors for the SM and the EFT contributions. To take into account detector effects, we include a flat detector efficiency which we deduce from the ratio of the predicted cross section and the predicted number of events provided by the experimental collaborations $\epsilon_{\text{det}} = N_{\text{events, pred}}/(\sigma_{\text{pred}} \mathcal{L}_{\text{int}})$.

WW production For WW production, we consider an asymmetry in the sine of the difference of the azimuthal angles ϕ of the two final state leptons ordered by their pseudorapidity, $\zeta_{W\gamma} = \Delta\phi_{\ell\ell}$. We make use of the existing RIVET [48] analysis to reproduce the experimental cuts and normalize the SHERPA cross section to the measured value of $\sigma_{\text{fid},EW} = 379.1 \pm 27.1$ fb [8]. The detector efficiency is deduced from the difference between the predicted cross section and the predicted number of events $\epsilon_{\text{det}} = 0.61$. Since the

signal-over-background ratio $S/B > 1$, we can safely neglect the uncertainty from background subtraction.

WZ production For WZ production, the CP-sensitive observable considered is $\zeta_{WZ} = \Delta\phi_{Z\ell'}$, where ℓ' denotes the lepton from the decay of the W boson and Z denotes the reconstructed Z boson from the same-flavor-opposite-sign lepton pair. We normalize the SHERPA cross section to the measured value of $\sigma_{\text{fid},EW} = 254.7 \pm 11.5$ fb [9] and assume a detector efficiency of $\epsilon_{\text{det}} = 0.52$. Since the signal-over-background ratio $S/B > 1$, we can safely neglect the background contributions.

W γ production For W γ production in the $\ell\nu\gamma$ final state we define the CP sensitive observable $\zeta_{W\gamma} = \Delta\phi_{\gamma\ell}$, where ℓ and γ denote the lepton from the W boson decay and of the photon, respectively. CMS has performed an analysis for W γ production at 13 TeV for an integrated luminosity of $\mathcal{L} = 127.1$ fb $^{-1}$ [10]. Including the decay of the W boson, the analysis has measured a cross section of $\sigma_{\text{fid}} = (3.32 \pm 0.16)$ pb. We implemented the experimental cuts in RIVET and normalized the cross section after cuts to this value. From the expected number of signal events and the expected cross section, we deduce a detector efficiency of $\epsilon_{\text{det}} = 0.59$. For W γ production, the signal-over-background ratio after cuts is $S/B \approx 0.54$ and we therefore explicitly take the uncertainty from background subtraction into consideration. Since the dominant background contributions arise from experimental effects such as nonprompt leptons and photons and e-induced photons, it is difficult to estimate their shape. For this reason, we assume the background shape to closely follow the signal shape in $\Delta\phi_{\gamma\ell}$.

Zjj production In vector boson fusion Zjj production, CP violation in the ZWW and γWW couplings causes modulations in the $\Delta\phi_{jj}$ distribution of the η -ordered jets, see Fig. 1. We normalize the SHERPA cross section to the measured value of $\sigma_{\text{fid},EW} = 37.4 \pm 6.5$ fb [11] and take into account a factor of $\epsilon_{\text{det}} = 0.85$ for detector effects. Since $S/B \approx 0.59$, we consider the uncertainty from background subtraction using the $\Delta\phi_{jj}$ distribution for the background as given in the experimental reference.

Wjj production For VBF Wjj production, we again base our analysis on the $\Delta\phi_{jj}$ distribution of the η -ordered jets. On top of the baseline selection used in Ref. [12], we apply a stricter cut on the invariant mass of the tagging jets $m_{jj} > 1100$ GeV, resulting in a signal-over-background ratio of $S/B \approx 0.13$. For the background, we have generated the dominant QCD Wjj contribution with SHERPA to obtain the shape. We normalize the event numbers to match the predicted number of total signal and background events in Ref. [12] rescaled by the luminosity.

Combination We combine the constraints on the Wilson coefficients from measurements of the WW, WZ, W γ , Zjj and Wjj channels in a χ^2 analysis. Since systematic uncertainties cancel out in our observables, we do not need to consider correlations between uncertainties of the different channels and directly calculate the χ^2 from the differential asymmetries A_{ij} via

$$\chi^2 = \sum_{i,j} \frac{(A_{ij} - 0.)^2}{\sigma_{A_{ij}}^2}, \quad (4)$$

$$i = WW, WZ, W\gamma, Zjj, Wjj, \quad j = 1, \dots, 6,$$

where $\sigma_{A_{ij}}$ denotes the combined statistical uncertainty from signal and background on the asymmetry in bin j of channel i . Given that the expected number of events is larger than 20 in all bins and for all considered channels, we can safely assume them to follow a Gaussian distribution.

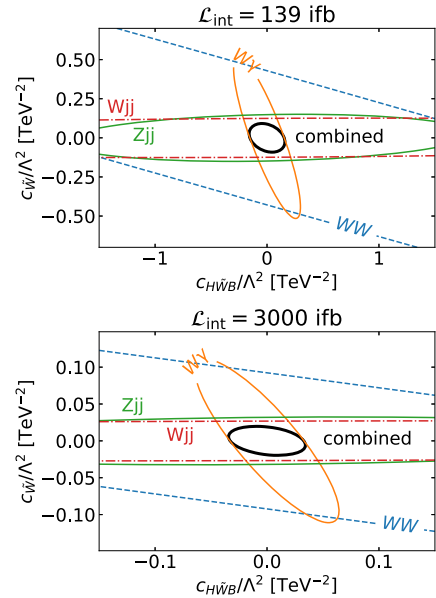


Fig. 3. Combination of the 95% CL limits from WW, WZ, W γ and Zjj production after LHC Run II ($\mathcal{L}_{\text{int}} = 139$ fb $^{-1}$, top) and after the HL-LHC ($\mathcal{L}_{\text{int}} = 3000$ fb $^{-1}$, bottom). The limits from WZ production are too weak to be visible in the plots.

We present the expected results for LHC Run II with an integrated luminosity of $\mathcal{L}_{\text{int}} = 139$ fb $^{-1}$ as well as prospects for the high luminosity LHC with an integrated luminosity $\mathcal{L}_{\text{int}} = 3000$ fb $^{-1}$ in Fig. 3. The strongest constraints result from W γ production for $c_{H\bar{W}B}$ and from the Zjj and Wjj channels for $c_{\bar{W}}$. Our bounds approximately agree with those presented in Ref. [30].² Some differences occur due to the inclusion of detector inefficiencies. For the W γ channel, we benefit from being able to recast an existing 13 TeV analysis rather than relying on assumptions for the cuts. Therefore, the cross section used for this channel is a factor 10 smaller in our analysis than assumed in Ref. [30].

Our limit on $c_{H\bar{W}B}$ is much stronger than the bound resulting from Higgs observables. At 3000 fb $^{-1}$ luminosity the expected limits are $|c_{H\bar{W}B}|/\Lambda^2 < 3.1$ TeV $^{-2}$ from Higgs WBF+ γ production [23] and $|c_{H\bar{W}B}|/\Lambda^2 < 1.5$ TeV $^{-2}$ from standard Higgs production processes [20] respectively compared to $|c_{H\bar{W}B}|/\Lambda^2 < 0.04$ TeV $^{-2}$ for this analysis of diboson observables. A fit combination of Higgs and diboson observables could in turn further improve the limits on other Wilson coefficients currently constrained from Higgs observables, $c_{H\bar{G}}$, $c_{H\bar{W}}$ and $c_{H\bar{B}}$. The Wilson coefficient of the operator $\mathcal{O}_{\bar{W}}$ is constrained to $|c_{\bar{W}}|/\Lambda^2 < 0.02$ TeV $^{-2}$ in our fit. High-luminosity LHC projections for diboson plus vector boson scattering data using distributions up to high- p_T instead of actual CP-sensitive observables find competitive constraints [29], further highlighting the necessity to combine fits of all available LHC data sets.

3. Neutral aTGCs

Neutral triple gauge couplings are absent in the SM at LO. Therefore, the observation of these couplings would be a clear hint for physics beyond the SM [49]. The most general parametrization of nTGCs in ZZ and Z γ production is given by [50], cf. also [35,51,52],

² Notice that our paper has a sign difference for the operator $c_{H\bar{W}B}$ with respect to Ref. [30] and Ref. [11]. We have validated our results by detailed comparison with MadGraph, with identical results. The one-parameter limits presented are not affected by the sign change.

$$\begin{aligned}
\mathcal{L} = \mathcal{L}_{\text{SM}} + \frac{e}{M_Z^2} \left[\right. \\
& - [f_4^\gamma (\partial_\mu F^{\mu\beta}) + f_4^Z (\partial_\mu Z^{\mu\beta})] Z_\alpha (\partial^\alpha Z_\beta) \\
& + [f_5^\gamma (\partial^\sigma F_{\sigma\mu}) + f_5^Z (\partial^\sigma Z_{\sigma\mu})] \tilde{Z}^{\mu\beta} Z_\beta \\
& - [h_1^\gamma (\partial^\sigma F_{\sigma\mu}) + h_1^Z (\partial^\sigma Z_{\sigma\mu})] Z_\beta F^{\mu\beta} \\
& - [h_3^\gamma (\partial_\sigma F^{\sigma\rho}) + h_3^Z (\partial_\sigma Z^{\sigma\rho})] Z^\alpha \tilde{F}_{\rho\alpha} \\
& - \frac{1}{M_Z^2} \left\{ h_2^\gamma [\partial_\alpha \partial_\beta \partial^\rho F_{\rho\mu}] + h_2^Z [\partial_\alpha \partial_\beta (\square + M_Z^2) Z_\mu] \right\} Z^\alpha F^{\mu\beta} \\
& \left. + \frac{1}{2M_Z^2} \left\{ h_4^\gamma [\square \partial^\sigma F^{\rho\alpha}] + h_4^Z [(\square + M_Z^2) \partial^\sigma Z^{\rho\alpha}] \right\} Z_\sigma \tilde{F}_{\rho\alpha} \right]. \tag{5}
\end{aligned}$$

Non-zero coefficients f_4^V , h_1^V and h_2^V lead to CP -violating interactions, while the coefficients f_5^V , h_3^V and h_4^V parametrize CP -conserving ZZZ , $ZZ\gamma$ and $Z\gamma\gamma$ interactions. In the SM, all h_i and f_i are zero at tree level. At the one-loop level, however, the CP -conserving couplings f_5 , h_3 and h_4 , receive non-zero contributions with relative sizes at the order of $\mathcal{O}(10^{-4})$ [53].

In contrast to charged TGCs, neutral TGCs can currently only be constrained to a regime where the quadratic terms clearly dominate over the linear interference terms with the SM, which are suppressed by the allowed polarizations of the gauge bosons. As a result, bounds on CP -violating neutral triple gauge couplings (nTGCs) stem primarily from their effect on the cross section in the high- p_T regime and they do not come from CP -sensitive observables [25,35,36]. In this section, we will therefore study the enhancement of relevant cross sections in high-momentum bins of kinematic distributions rather than CP asymmetries. In particular, we will study the high- p_T regime of the distributions of $p_T^{\ell\ell}$ in ZZ production as well as $E_{T,\gamma}$ in $Z\gamma$ production. Bounds on nTGCs have previously been discussed for the LHC [25,35,36,54] as well as for future lepton [55,56] and proton colliders [57–59]. Since both the bounds on the coefficients of CP -violating interactions and their CP -conserving counterparts ($f_4^V \leftrightarrow f_5^V$, $h_1^V \leftrightarrow h_3^V$, $h_2^V \leftrightarrow h_4^V$) result from their quadratic effect on the cross section in the high- p_T regime, their limits are typically very similar.

Neutral triple gauge couplings do not appear at the dimension-six level in the SMEFT. They are, however, induced at dimension-eight [54] (f_4^V , f_5^V , h_1^V , h_3^V) or even higher dimension. While an interpretation of nTGCs in SMEFT at dimension-eight is therefore possible, the clear dominance of the quadratic terms over the dimension-eight interference terms renders the interpretation cumbersome and possibly flawed. Consequently, we will rely on the parametrization given in Eq. (5).

Events for the analysis of neutral anomalous gauge couplings are generated at leading order using the native SM+AGC model in SHERPA-2.1.1 [37] as well as an implementation in a UFO model [38, 47,60]. Event generation includes both the suppressed and mostly negligible interference with the SM model as well as the squared nTGC contributions.

ZZ production We study ZZ production in its leptonic 4ℓ [31] and $2\ell 2\nu$ [32] final states. The measured cross sections in the fiducial regions of these channels are $\sigma_{4\ell} = (46.2 \pm 2.4)$ fb [31] and $\sigma_{2\ell 2\nu} = (25.4 \pm 1.7)$ fb [32], respectively. In both cases, we use the $p_T^{\ell\ell}$ distributions to constrain the nTGC; in the 4ℓ final state we use the two leptons of the leading reconstructed Z boson. To facilitate direct comparison with published data, we employ the binning used by the experimental collaborations for their luminosity projections.

In our event generation, we include the LO gg and qq initial state contributions for ZZ production. The effect of nTGCs is, however, only included for the qq initial state which makes up for about 90% of the total number of events. NNLO QCD and NLO EW

Table 1

Expected limits on nTGCs for the combination of the $ZZ \rightarrow 4\ell$ and $ZZ \rightarrow 2\ell 2\nu$ analyses at different luminosities. The limits on the parameters f_5^V which lead to CP -conserving interactions are equivalent to those on their CP -violating counterparts. In the two bottom rows, we present the limits assuming that the relative systematic uncertainties in each bin have been halved with respect to the value quoted by the experimental collaborations at 36.1 fb^{-1} .

lumi [fb^{-1}]	$ f_4^\gamma \cdot 10^4$	$ f_4^Z \cdot 10^4$
139	11.	9.1
300	9.1	7.7
3000	7.2	6.1
300 ($\sigma_{\text{syst}}/2$)	8.2	7.0
3000 ($\sigma_{\text{syst}}/2$)	5.3	4.5

corrections for the events are included through bin-by-bin k factors, assuming the same values for SM and BSM contributions. These are deduced from the ratio of the LO results with respect to the most precise SHERPA prediction available. The total number of events in each bin i is given by $N_i^{\text{SHERPA}} = N_i^{qq} + N_i^{gg} = \epsilon_i^{\text{det}} \mathcal{L}_{\text{int}} (\sigma_i^{qq, \text{NLO}} + 1.67 \sigma_i^{gg})$, where the gg contribution is corrected by a relative k factor of 1.67. Detector effects are accounted for through bin-by-bin detector efficiency factors ϵ_i^{det} for the 4ℓ final state (ranging between 0.57 and 0.69) by comparing the expected cross sections with the expected number of events in each bin. For the $2\ell 2\nu$ analysis, where the unfolded cross section is given in the experimental reference, we use a global detector efficiency of $\epsilon^{\text{det}} = 0.57$.

To set limits on the nTGCs, we perform a χ^2 analysis for each bin in the two available $p_T^{\ell\ell}$ distributions,

$$\chi^2 = \sum_{i \in \text{bins}} \frac{(N_i^{\text{data}} - N_i^{\text{pred}})^2}{N_i^{\text{data}} + (\sigma_i^{\text{syst}})^2}, \tag{6}$$

where N_i^{data} and N_i^{pred} denote the number of observed and predicted events in each bin and σ_i^{syst} is their systematic uncertainty. For both analysis channels, the constraints on nTGCs stem almost entirely from the last bin, i.e. $p_T^{\ell\ell} \in [555, 3000]$ GeV in 4ℓ final state and $p_T^{\ell\ell} \in [350, 1000]$ GeV in the $2\ell 2\nu$ final state.

To validate our analysis, we have explicitly checked that we can reproduce the limits on f_i^V presented by the experimental collaborations [31,32] for a luminosity of 36.1 fb^{-1} at the 15% level. Deviations from those limits can be fully explained by the use of different Monte Carlo generators and the fact that we only know the global detector acceptance rather than a bin-by-bin value for the $2\ell 2\nu$ final state.

Combining the limits from the 4ℓ and $2\ell 2\nu$ final states for a luminosity of 3000 fb^{-1} , we find 95% CL bounds of

$$|f_4^\gamma| < 7.2 \cdot 10^{-4}, \quad |f_4^Z| < 6.1 \cdot 10^{-4}, \tag{7}$$

for the parameters inducing CP -violating interactions when constraining one parameter at a time. Since the linear interference contributions are not statistically relevant, we display the limit on the absolute values of the parameters instead of presenting separated upper and lower 95% CL limits. We collect projected limits at different luminosities in Table 1. As expected, the limits on the parameters f_5^V which lead to CP -conserving interactions are equivalent to those of its CP -violating counterparts f_4^V . Our combined 139 fb^{-1} limits approximately agree with those found by CMS for LHC Run-II in the 4ℓ final state [61], which however draws most of its sensitivity from an overflow bin, $m_{ZZ} > 1300$ GeV.

Had we included the overflow in the last bin instead of keeping to the binning used by the experimental collaborations, the obtained limits would have tightened by $\lesssim 20\%$. We generally avoid including the overflow in our last bins, however, to make sure that

Table 2

Expected limits on nTGCs for the combination of the $Z\gamma \rightarrow 2\ell\gamma$ and $Z\gamma \rightarrow 2\nu\gamma$ analyses at different luminosities. In the two bottom rows, we present the limits assuming that the relative systematic uncertainties in each bin have been halved with respect to the value quoted by the experimental collaborations.

lumi [fb ⁻¹]	10 ⁴ h ₁ ^γ	10 ⁴ h ₁ ^Z	10 ⁷ h ₂ ^γ	10 ⁷ h ₂ ^Z
139	3.6	3.2	8.1	8.1
300	3.2	2.9	7.3	7.2
3000	2.7	2.4	6.1	6.1
300 (σ _{syst} /2)	2.7	2.4	6.1	6.1
3000 (σ _{syst} /2)	2.0	1.8	4.5	4.4

all considered events lie in a kinematic regime for which the detector is well understood. In addition, using constrained last bins circumvents potential issues when translating the limits to other frameworks such as EFTs.

Zγ production We study $Z\gamma$ production in the leptonic $2\ell\gamma$ [33] and $2\nu\gamma$ final states [34] to constrain the CP -odd interactions induced by h_1^V and h_2^V , compare Eq. (5). The measured inclusive cross section for $2\ell\gamma$ final state is $\sigma_{2\ell\gamma} = (1065.4 \pm 23.5)$ fb [33]. For the analysis of the $2\nu\gamma$ final state which vetoes additional jets, the measured cross section is $\sigma_{2\nu\gamma} = (52.4 \pm 4.8)$ fb [34]. We assume a detector efficiency of $\epsilon_{2\ell\gamma}^{\text{det}} = 0.54$ for the $2\ell\gamma$ channel and $\epsilon_{2\nu\gamma}^{\text{det}} = 0.89$ for the $2\nu\gamma$ channel. NNLO QCD and NLO EW corrections are again included through bin-by-bin k factors by rescaling to the predictions in Refs. [33,34].

To calculate and combine the limits from $Z\gamma$, we again add up χ^2 for each bin in the $E_{T,\gamma}$ distribution, see Eq. (6), using the binning given in the corresponding experimental references excluding overflow bins. Our last bins, which have the greatest sensitivity to the nTGCs, range from $E_{T,\gamma} \in [500, 1200]$ GeV for $2\ell\gamma$ and $E_{T,\gamma} \in [600, 1100]$ GeV for the $2\nu\gamma$ analysis. As we will point out below, including the overflow in the last bin has a severe impact on the limits on h_2^V . To validate our analysis, we have explicitly checked that we can reproduce the expected limits of the analysis of the $2\nu\gamma$ final state at a luminosity of 36.1 fb^{-1} [34] when including the overflow in the last bin.

Combining the limits from the $2\ell\gamma$ and $2\nu\gamma$ final states for a luminosity of 3000 fb^{-1} , we find 95% CL one-parameter bounds of

$$\begin{aligned} |h_1^\gamma| < 2.7 \cdot 10^{-4}, \quad |h_1^Z| < 2.4 \cdot 10^{-4}, \\ |h_2^\gamma| < 6.1 \cdot 10^{-7}, \quad |h_2^Z| < 6.1 \cdot 10^{-7}, \end{aligned} \quad (8)$$

for the CP -odd nTGCs. These values assume the same relative systematic uncertainties as in the experimental references at 36.1 fb^{-1} and 139 fb^{-1} . Including the overflow in the last bin, the limits on h_1^V tighten by $\sim 20\%$. On the other hand, the limits on h_2^V are much more severely affected; they are approximately halved when including the overflow in the last bin. This implies that care has to be taken when translating limits based on an analysis including the overflow bin such as Ref. [34] into, for instance, an EFT framework. We collect the limits for other luminosities in Table 2. Since for higher luminosities and a fixed binning the uncertainty on the last bin quickly becomes dominated by systematic effects, we also present limits assuming systematic uncertainties are reduced by a factor of two. Because the limits on CP -even nTGCs are roughly equivalent to those on their CP -odd counterparts we do not present them explicitly here.

4. Conclusions and outlook

We have studied the constraints on CP -odd anomalous triple gauge couplings from diboson production.

For the TGCs involving W bosons, we have analysed differential asymmetries in CP -sensitive observables based on $\Delta\phi$ and present

our results in the SMEFT framework at dimension-six. Marginalizing over the second Wilson coefficient, we can constrain the coefficients to $|c_{H\bar{W}B}|/\Lambda^2 < 0.04 \text{ TeV}^{-2}$ and $|c_{\bar{W}}|/\Lambda^2 < 0.02 \text{ TeV}^{-2}$ at 3000 fb^{-1} . The strongest limits stem from the analysis of $W\gamma$, Wjj and Zjj production. The improved limits on the coefficient $c_{H\bar{W}B}$ with respect to limits resulting from Higgs observables, motivates a combination of Higgs, vector boson scattering and diboson data for a combined fit of CP -violating operators.

To constrain neutral triple gauge couplings, we combined the bounds from the leptonic decay channels of ZZ and $Z\gamma$ production. The most severe limits are obtained from the high- p_T regimes of differential distributions instead of CP -sensitive observables due to vanishingly small SM–New Physics interference terms. The resulting combined limits on CP -odd interactions at 3000 fb^{-1} are $|f_4^Z| < 7.2 \cdot 10^{-4}$, $|f_4^\gamma| < 6.1 \cdot 10^{-4}$ from ZZ production and $|h_1^\gamma| < 2.7 \cdot 10^{-4}$, $|h_1^Z| < 2.4 \cdot 10^{-4}$, $|h_2^\gamma|$, $|h_2^Z| < 6.1 \cdot 10^{-7}$ from $Z\gamma$ production. Limits on h_2^V are significantly tighter when including the overflow above $\sim 1 \text{ TeV}$ in the last bin. This should be taken into account when translating these limits to an EFT framework.

In summary, we presented expected limits on CP -odd anomalous triple gauge couplings for future runs of the LHC and thereby provided bounds on additional sources of CP -violation in the SM.

Declaration of competing interest

The authors declare that they have no known competing financial interests or personal relationships that could have appeared to influence the work reported in this paper.

Acknowledgements

PG, FK and MS are supported by the UK Science and Technology Facilities Council (STFC) under grant ST/P001246/1. AB gratefully acknowledges support from the Alexander von Humboldt Foundation as a Feodor Lynen Fellow. FK and MS are acknowledging support from the European Union's Horizon 2020 research and innovation programme as part of the Marie Skłodowska-Curie Innovative Training Network MCnetITN3 (grant agreement no. 722104). MS is funded by the Royal Society through a University Research Fellowship (URF\R1\180549), and FK gratefully acknowledges support by the Wolfson Foundation and the Royal Society under award RSWF\R1\191029.

References

- [1] G. Aad, et al., Observation of a new particle in the search for the Standard Model Higgs boson with the ATLAS detector at the LHC, Phys. Lett. B 716 (2012) 1–29, <https://doi.org/10.1016/j.physletb.2012.08.020>, arXiv:1207.7214.
- [2] S. Chatrchyan, et al., Observation of a new boson at a mass of 125 GeV with the CMS experiment at the LHC, Phys. Lett. B 716 (2012) 30–61, <https://doi.org/10.1016/j.physletb.2012.08.021>, arXiv:1207.7235.
- [3] A.D. Sakharov, Violation of CP invariance, C asymmetry, and baryon asymmetry of the universe, Pisma Zh. Eksp. Teor. Fiz. 5 (1967) 32–35, JETP Lett. 5 (1967) 24, Sov. Phys. Usp. 34 (5) (1991) 392, Usp. Fiz. Nauk 161 (5) (1991) 61, <https://doi.org/10.1070/PU1991v034n05ABEH002497>.
- [4] V.A. Kuzmin, V.A. Rubakov, M.E. Shaposhnikov, On the anomalous electroweak baryon number nonconservation in the early universe, Phys. Lett. B 155 (1985) 36, [https://doi.org/10.1016/0370-2693\(85\)91028-7](https://doi.org/10.1016/0370-2693(85)91028-7).
- [5] M.E. Shaposhnikov, Baryon asymmetry of the universe in standard electroweak theory, Nucl. Phys. B 287 (1987) 757–775, [https://doi.org/10.1016/0550-3213\(87\)90127-1](https://doi.org/10.1016/0550-3213(87)90127-1).
- [6] A.E. Nelson, D.B. Kaplan, A.G. Cohen, Why there is something rather than nothing: matter from weak interactions, Nucl. Phys. B 373 (1992) 453–478, [https://doi.org/10.1016/0550-3213\(92\)90440-M](https://doi.org/10.1016/0550-3213(92)90440-M).
- [7] D.E. Morrissey, M.J. Ramsey-Musolf, Electroweak baryogenesis, New J. Phys. 14 (2012) 125003, <https://doi.org/10.1088/1367-2630/14/12/125003>, arXiv:1206.2942.
- [8] M. Aaboud, et al., Measurement of fiducial and differential W^+W^- production cross-sections at $\sqrt{s} = 13 \text{ TeV}$ with the ATLAS detector, Eur. Phys. J.

- C 79 (10) (2019) 884, <https://doi.org/10.1140/epjc/s10052-019-7371-6>, arXiv:1905.04242.
- [9] M. Aaboud, et al., Search for resonant WZ production in the fully leptonic final state in proton-proton collisions at $\sqrt{s} = 13$ TeV with the ATLAS detector, *Phys. Lett. B* 787 (2018) 68–88, <https://doi.org/10.1016/j.physletb.2018.10.021>, arXiv:1806.01532.
- [10] Measurement of the inclusive $W\gamma$ production cross section in proton-proton collisions at $\sqrt{s} = 13$ TeV and constraints on effective field theory, 2020.
- [11] G. Aad, et al., Differential cross-section measurements for the electroweak production of dijets in association with a Z boson in proton-proton collisions at ATLAS, *Eur. Phys. J. C* 81 (2) (2021) 163, <https://doi.org/10.1140/epjc/s10052-020-08734-w>, arXiv:2006.15458.
- [12] A.M. Sirunyan, et al., Measurement of electroweak production of a W boson in association with two jets in proton-proton collisions at $\sqrt{s} = 13$ TeV, *Eur. Phys. J. C* 80 (1) (2020) 43, <https://doi.org/10.1140/epjc/s10052-019-7585-7>, arXiv:1903.04040.
- [13] W. Buchmuller, D. Wyler, Effective Lagrangian analysis of new interactions and flavor conservation, *Nucl. Phys. B* 268 (1986) 621–653, [https://doi.org/10.1016/0550-3213\(86\)90262-2](https://doi.org/10.1016/0550-3213(86)90262-2).
- [14] H. Georgi, Effective field theory, *Annu. Rev. Nucl. Part. Sci.* 43 (1993) 209–252, <https://doi.org/10.1146/annurev.ns.43.120193.001233>.
- [15] B. Grzadkowski, M. Iskrzynski, M. Misiak, J. Rosiek, Dimension-six terms in the Standard Model Lagrangian, *J. High Energy Phys.* 10 (2010) 085, [https://doi.org/10.1007/JHEP10\(2010\)085](https://doi.org/10.1007/JHEP10(2010)085), arXiv:1008.4884.
- [16] R. Alonso, E.E. Jenkins, A.V. Manohar, M. Trott, Renormalization group evolution of the Standard Model dimension six operators III: gauge coupling dependence and phenomenology, *J. High Energy Phys.* 04 (2014) 159, [https://doi.org/10.1007/JHEP04\(2014\)159](https://doi.org/10.1007/JHEP04(2014)159), arXiv:1312.2014.
- [17] I. Brivio, M. Trott, The Standard Model as an effective field theory, *Phys. Rep.* 793 (2019) 1–98, <https://doi.org/10.1016/j.physrep.2018.11.002>, arXiv:1706.08945.
- [18] F. Ferreira, B. Fuks, V. Sanz, D. Sengupta, Probing CP -violating Higgs and gauge-boson couplings in the Standard Model effective field theory, *Eur. Phys. J. C* 77 (10) (2017) 675, <https://doi.org/10.1140/epjc/s10052-017-5226-6>, arXiv:1612.01808.
- [19] J. Brehmer, F. Kling, T. Plehn, T.M.P. Tait, Better Higgs- CP tests through information geometry, *Phys. Rev. D* 97 (9) (2018) 095017, <https://doi.org/10.1103/PhysRevD.97.095017>, arXiv:1712.02350.
- [20] F.U. Bernlochner, C. Englert, C. Hays, K. Lohwasser, H. Mildner, A. Pilkington, D.D. Price, M. Spannowsky, Angles on CP -violation in Higgs boson interactions, *Phys. Lett. B* 790 (2019) 372–379, <https://doi.org/10.1016/j.physletb.2019.01.043>, arXiv:1808.06577.
- [21] C. Englert, P. Galler, A. Pilkington, M. Spannowsky, Approaching robust EFT limits for CP -violation in the Higgs sector, *Phys. Rev. D* 99 (9) (2019) 095007, <https://doi.org/10.1103/PhysRevD.99.095007>, arXiv:1901.05982.
- [22] V. Cirigliano, A. Crivellin, W. Dekens, J. de Vries, M. Hofferichter, E. Mereghetti, CP violation in Higgs-gauge interactions: from tabletop experiments to the LHC, *Phys. Rev. Lett.* 123 (5) (2019) 051801, <https://doi.org/10.1103/PhysRevLett.123.051801>, arXiv:1903.03625.
- [23] A. Biekötter, R. Gomez-Ambrosio, P. Gregg, F. Krauss, M. Schönherr, Constraining SMEFT operators with associated $h\gamma$ production in Weak Boson Fusion, *Phys. Lett. B* 814 (2021) 136079, <https://doi.org/10.1016/j.physletb.2021.136079>, arXiv:2003.06379.
- [24] J. Kumar, A. Rajaraman, J.D. Wells, Probing CP -violation at colliders through interference effects in diboson production and decay, *Phys. Rev. D* 78 (2008) 035014, <https://doi.org/10.1103/PhysRevD.78.035014>, arXiv:0801.2891.
- [25] S. Dawson, S.K. Gupta, G. Valencia, CP violating anomalous couplings in $W\gamma$ and $Z\gamma$ production at the LHC, *Phys. Rev. D* 88 (3) (2013) 035008, <https://doi.org/10.1103/PhysRevD.88.035008>, arXiv:1304.3514.
- [26] M.B. Gavela, J. Gonzalez-Fraile, M.C. Gonzalez-Garcia, L. Merlo, S. Rigolin, J. Yepes, CP violation with a dynamical Higgs, *J. High Energy Phys.* 10 (2014) 044, [https://doi.org/10.1007/JHEP10\(2014\)044](https://doi.org/10.1007/JHEP10(2014)044), arXiv:1406.6367.
- [27] A. Azatov, D. Barducci, E. Venturini, Precision diboson measurements at hadron colliders, *J. High Energy Phys.* 04 (2019) 075, [https://doi.org/10.1007/JHEP04\(2019\)075](https://doi.org/10.1007/JHEP04(2019)075), arXiv:1901.04821.
- [28] R. Rahaman, R.K. Singh, Unravelling the anomalous gauge boson couplings in ZW^\pm production at the LHC and the role of spin-1 polarizations, *J. High Energy Phys.* 04 (2020) 075, [https://doi.org/10.1007/JHEP04\(2020\)075](https://doi.org/10.1007/JHEP04(2020)075), arXiv:1911.03111.
- [29] J.J. Ethier, R. Gomez-Ambrosio, G. Magni, J. Rojo, SMEFT analysis of vector boson scattering and diboson data from the LHC Run II, arXiv:2101.03180, 2021.
- [30] S. Das Bakshi, J. Chakraborty, C. Englert, M. Spannowsky, P. Stylianou, CP violation at ATLAS in effective field theory, *Phys. Rev. D* 103 (5) (2021) 055008, <https://doi.org/10.1103/PhysRevD.103.055008>, arXiv:2009.13394.
- [31] M. Aaboud, et al., $ZZ \rightarrow \ell^+ \ell^- \ell'^+ \ell'^-$ cross-section measurements and search for anomalous triple gauge couplings in 13 TeV pp collisions with the ATLAS detector, *Phys. Rev. D* 97 (3) (2018) 032005, <https://doi.org/10.1103/PhysRevD.97.032005>, arXiv:1709.07703.
- [32] M. Aaboud, et al., Measurement of ZZ production in the $\ell\ell\nu\nu$ final state with the ATLAS detector in pp collisions at $\sqrt{s} = 13$ TeV, *J. High Energy Phys.* 10 (2019) 127, [https://doi.org/10.1007/JHEP10\(2019\)127](https://doi.org/10.1007/JHEP10(2019)127), arXiv:1905.07163.
- [33] G. Aad, et al., Measurement of the $Z(\rightarrow \ell^+ \ell^-) \gamma$ production cross-section in pp collisions at $\sqrt{s} = 13$ TeV with the ATLAS detector, *J. High Energy Phys.* 03 (2020) 054, [https://doi.org/10.1007/JHEP03\(2020\)054](https://doi.org/10.1007/JHEP03(2020)054), arXiv:1911.04813.
- [34] M. Aaboud, et al., Measurement of the $Z\gamma \rightarrow \nu\bar{\nu}\gamma$ production cross section in pp collisions at $\sqrt{s} = 13$ TeV with the ATLAS detector and limits on anomalous triple gauge-boson couplings, *J. High Energy Phys.* 12 (2018) 010, [https://doi.org/10.1007/JHEP12\(2018\)010](https://doi.org/10.1007/JHEP12(2018)010), arXiv:1810.04995.
- [35] U. Baur, E.L. Berger, Probing the weak boson sector in $Z\gamma$ production at hadron colliders, *Phys. Rev. D* 47 (1993) 4889–4904, <https://doi.org/10.1103/PhysRevD.47.4889>.
- [36] R. Rahaman, R.K. Singh, Anomalous triple gauge boson couplings in ZZ production at the LHC and the role of Z boson polarizations, *Nucl. Phys. B* 948 (2019) 114754, <https://doi.org/10.1016/j.nuclphysb.2019.114754>, arXiv:1810.11657.
- [37] T. Gleisberg, S. Höche, F. Krauss, M. Schönherr, S. Schumann, F. Siegert, J. Winter, Event generation with SHERPA 1.1, *J. High Energy Phys.* 02 (2009) 007, <https://doi.org/10.1088/1126-6708/2009/02/007>, arXiv:0811.4622.
- [38] E. Bothmann, et al., Event generation with Sherpa 2.2, *SciPost Phys.* 7 (3) (2019) 034, <https://doi.org/10.21468/SciPostPhys.7.3.034>, arXiv:1905.09127.
- [39] R.D. Ball, et al., Parton distributions for the LHC Run II, *J. High Energy Phys.* 04 (2015) 040, [https://doi.org/10.1007/JHEP04\(2015\)040](https://doi.org/10.1007/JHEP04(2015)040), arXiv:1410.8849.
- [40] A. Buckley, J. Ferrando, S. Lloyd, K. Nordström, B. Page, M. Rüfenacht, M. Schönherr, G. Watt, LHAPDF6: parton density access in the LHC precision era, *Eur. Phys. J. C* 75 (2015) 132, <https://doi.org/10.1140/epjc/s10052-015-3318-8>, arXiv:1412.7420.
- [41] T. Gleisberg, S. Höche, Comix, a new matrix element generator, *J. High Energy Phys.* 12 (2008) 039, <https://doi.org/10.1088/1126-6708/2008/12/039>, arXiv:0808.3674.
- [42] S. Schumann, F. Krauss, A parton shower algorithm based on Catani-Seymour dipole factorisation, *J. High Energy Phys.* 03 (2008) 038, <https://doi.org/10.1088/1126-6708/2008/03/038>, arXiv:0709.1027.
- [43] D.R. Yennie, S.C. Frautschi, H. Suura, The infrared divergence phenomena and high-energy processes, *Ann. Phys.* 13 (1961) 379–452, [https://doi.org/10.1016/0003-4916\(61\)90151-8](https://doi.org/10.1016/0003-4916(61)90151-8).
- [44] M. Schönherr, F. Krauss, Soft photon radiation in particle decays in SHERPA, *J. High Energy Phys.* 12 (2008) 018, <https://doi.org/10.1088/1126-6708/2008/12/018>, arXiv:0810.5071.
- [45] I. Brivio, Y. Jiang, M. Trott, The SMEFTsim package, theory and tools, *J. High Energy Phys.* 12 (2017) 070, [https://doi.org/10.1007/JHEP12\(2017\)070](https://doi.org/10.1007/JHEP12(2017)070), arXiv:1709.06492.
- [46] C. Degrande, C. Duhr, B. Fuks, D. Grellscheid, O. Mattelaer, T. Reiter, UFO - the universal FeynRules output, *Comput. Phys. Commun.* 183 (2012) 1201–1214, <https://doi.org/10.1016/j.cpc.2012.01.022>, arXiv:1108.2040.
- [47] S. Höche, S. Kuttimalai, S. Schumann, F. Siegert, Beyond Standard Model calculations with Sherpa, *Eur. Phys. J. C* 75 (3) (2015) 135, <https://doi.org/10.1140/epjc/s10052-015-3338-4>, arXiv:1412.6478.
- [48] A. Buckley, J. Butterworth, L. Lonnblad, D. Grellscheid, H. Hoeth, J. Monk, H. Schulz, F. Siegert, Rivet user manual, *Comput. Phys. Commun.* 184 (2013) 2803–2819, <https://doi.org/10.1016/j.cpc.2013.05.021>, arXiv:1003.0694.
- [49] T. Corbett, M.J. Dolan, C. Englert, K. Nordström, Anomalous neutral gauge boson interactions and simplified models, *Phys. Rev. D* 97 (11) (2018) 115040, <https://doi.org/10.1103/PhysRevD.97.115040>, arXiv:1710.07530.
- [50] G.J. Gounaris, J. Layssac, F.M. Renard, Signatures of the anomalous Z_γ and ZZ production at the lepton and hadron colliders, *Phys. Rev. D* 61 (2000) 073013, <https://doi.org/10.1103/PhysRevD.61.073013>, arXiv:hep-ph/9910395.
- [51] K. Hagiwara, R. Peccei, D. Zeppenfeld, K. Hikasa, Probing the weak boson sector in $e^+e^- \rightarrow W^+W^-$, *Nucl. Phys. B* 282 (1987) 253–307, [https://doi.org/10.1016/0550-3213\(87\)90685-7](https://doi.org/10.1016/0550-3213(87)90685-7).
- [52] U. Baur, D.L. Rainwater, Probing neutral gauge boson selfinteractions in ZZ production at the Tevatron, *Int. J. Mod. Phys. A* 16S1A (2001) 315–317, <https://doi.org/10.1142/S0217751X01006796>, arXiv:hep-ph/0011016.
- [53] G.J. Gounaris, J. Layssac, F.M. Renard, New and standard physics contributions to anomalous Z and gamma selfcouplings, *Phys. Rev. D* 62 (2000) 073013, <https://doi.org/10.1103/PhysRevD.62.073013>, arXiv:hep-ph/0003143.
- [54] C. Degrande, A basis of dimension-eight operators for anomalous neutral triple gauge boson interactions, *J. High Energy Phys.* 02 (2014) 101, [https://doi.org/10.1007/JHEP02\(2014\)101](https://doi.org/10.1007/JHEP02(2014)101), arXiv:1308.6323.
- [55] R. Rahaman, R.K. Singh, On polarization parameters of spin-1 particles and anomalous couplings in $e^+e^- \rightarrow ZZ/Z\gamma$, *Eur. Phys. J. C* 76 (10) (2016) 539, <https://doi.org/10.1140/epjc/s10052-016-4374-4>, arXiv:1604.06677.
- [56] J. Ellis, S.-F. Ge, H.-J. He, R.-Q. Xiao, Probing the scale of new physics in the $ZZ\gamma$ coupling at e^+e^- colliders, *Chin. Phys. C* 44 (6) (2020) 063106, <https://doi.org/10.1088/1674-1137/44/6/063106>, arXiv:1902.06631.
- [57] A. Yilmaz, A. Senol, H. Denizli, I. Turk Cakir, O. Cakir, Sensitivity on anomalous neutral triple gauge couplings via ZZ production at FCC-hh, *Eur. Phys. J. C* 80 (2) (2020) 173, <https://doi.org/10.1140/epjc/s10052-020-7731-2>, arXiv:1906.03911.
- [58] A. Senol, H. Denizli, A. Yilmaz, I. Turk Cakir, O. Cakir, Study on anomalous neutral triple gauge boson couplings from dimension-eight operators at the HL-LHC, arXiv:1906.04589, <https://doi.org/10.5506/APhysPolB.50.1597>, 2019.

- [59] J. Ellis, H.-J. He, R.-Q. Xiao, Probing new physics in dimension-8 neutral gauge couplings at e^+e^- colliders, *Sci. China, Phys. Mech. Astron.* 64 (2) (2021) 221062, <https://doi.org/10.1007/s11433-020-1617-3>, arXiv:2008.04298.
- [60] S. Banerjee, private communication.
- [61] A.M. Sirunyan, et al., Measurements of $pp \rightarrow ZZ$ production cross sections and constraints on anomalous triple gauge couplings at $\sqrt{s} = 13$ TeV, *Eur. Phys. J. C* 81 (3) (2021) 200, <https://doi.org/10.1140/epjc/s10052-020-08817-8>, arXiv:2009.01186.